JOURNAL OF MATERIALS SCIENCE 32 (1997) 6625–6628

Cathodoluminescence microscopy of impurity phases in ZrO_2/Ni nano–composites

A. GHOLINIA, C. LEACH
Manchester Materials Science Centre, University of Manchester & UMIST, Grosvenor Street, Manchester, M1 7HS, UK

Cathodoluminescence (CL) microscopy of Ni/cubic-ZrO_2 nano–composites has been used to demonstrate the presence of both secondary phases and compositional fluctuations within the microstructure. X-ray microanalysis showed that in this material red CL emissions were generated from aluminium rich phases, blue emissions originated from silicon rich phases, and green CL emissions were associated with a monoclinic zirconia phase. In rapidly characterizing the distribution and density of these impurities, the CL technique has proved to be a powerful and versatile tool in the determination of the purity of sintered pellets.

1. Introduction

The inherent brittleness of ceramic materials can be compensated to a certain extent by the inclusion of plastic phases, such as metals, to form a duplex structure [1, 2]. During fracture the metal phase can absorb energy in deforming plastically and thus increase the toughness of the material [3]. Nano–cermets may also show benefits in other areas, such as improved homogeneity of electrical properties. Porous Ni/ZrO_2 nano–composites for example are candidate materials for the first generation of solid oxide fuel cell anode/current collecter assemblies.

Sol–gel preparation techniques are known to produce powders that give rise to well-distributed metal particles in a nano–composite on sintering, but optimization of the required properties can only be carried out if the final microstructure is closely controlled and free from randomly distributed unwanted phases. Cathodoluminescence (CL) microscopy can provide useful information in this regard about microstructural inhomogeneities that may affect both the mechanical and electrical properties of the material [4].

CL microscopy is a relatively underexploited characterization method for the study of ceramics and other wide band gap materials. It has been used extensively to study geological [5] and semiconductor materials [6, 7]. The detection sensitivity of certain elements by CL analysis can be 10^4 times better than that attainable by X-ray microanalysis. In the right circumstances impurity concentrations as low as 10^{14} atoms cm^{-3} can be detected [7].

Examples of CL microscopy of ceramics include studies of zirconia phase transformations [8, 9] and high T_c superconductors where impurity phase distributions in targets used for laser ablation of superconducting thin films were studied [4]. CL microscopy has also been used to assess the quality of single crystal MgO substrate materials for thin film deposition [10].

CL microscopy involves the analysis of light emissions that occur by electron–hole pair recombination between quantum states in the energy band structure. The electron–hole pairs are generated by the bombardment of a sample by an energetic electron beam. In wide bandgap materials, additional states need to be generated within the bandgap to support transitions in the visible range. Luminescence can also be generated by exciting states internal to an ion. Such self luminescent centres, which are typically transition metals, give characteristic spectral responses modified only slightly by the ligand field. If this is the case, the wavelength and intensity of the light emissions can be used to characterize the material and the distribution of certain impurities within it.

2. Experimental procedure

Duplex Ni–ZrO_2 nano–composites containing 30 wt % nickel and 15 wt % yttria were fabricated using the sol–gel technique [11]. The powders were calcined at 600°C for 5 h in oxygen after which there was a further treatment at 1100°C in hydrogen for 5 h to reduce any nickel oxide in the microstructure to the metallic state. Compacts were cold isostatically pressed at 300MPa and then sintered by uniaxial hot pressing at 60MPa and 1000°C for up to 2 h in argon. The surface of the pellet was ground, polished and ultrasonically cleaned prior to the CL analysis.

Panchromatic optical-CL images of the sample were recorded in colour on a light microscope using a Technosyn model CCL8200 Mark3 cold cathode luminescence stage operated at 10–15 kV and a load current of 300–400 μA which resulted in approximately 1 cm^2 of the sample surface being illuminated (Fig. 1).

The secondary electron (SE) and scanning electron microscope-CL (SEM-CL) images were obtained using a Jeol 6400 SEM, operating at 15 kV and 15 nA

0022–2461

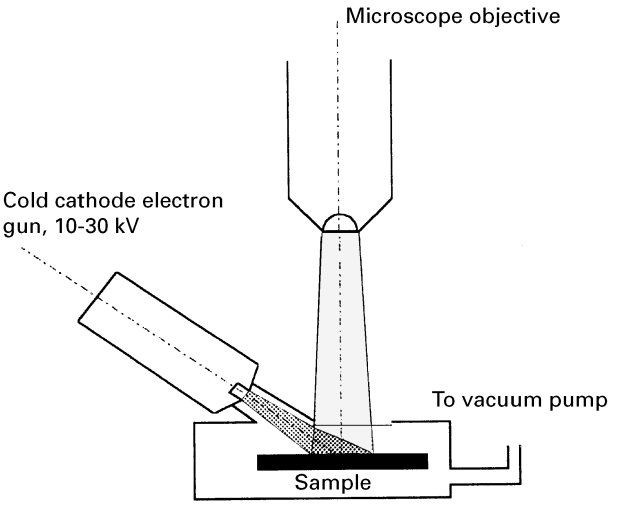

Figure 1 Schematic diagram of the optical CL system used in this study.

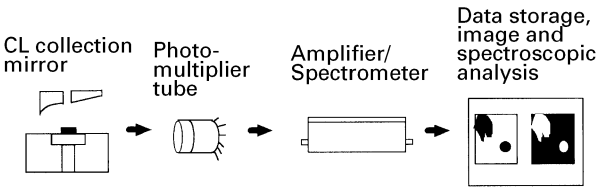

Figure 2 Schematic diagram of the SEM-CL system used in this study.

beam current. The penetration depth at this kV is about 0.7 μm and there was therefore the possibility of correlating luminescent centres with individual grains or other features visible at the surface. Fig. 2 is a schematic diagram of the SEM based CL detection system. Energy-dispersive X-rays (EDX) microanalysis, consisting of traverses and point analyses, was carried out on a Philips 505 scanning electron microscope fitted with an EDAX 9100 system.

3. Results and discussion

Fig. 3 shows a typical optical CL image of a polished surface of the hot pressed Ni/cubic-ZrO_2 nano-composite. Red, blue and green spots are clearly visible, randomly distributed at points on the surface of the pellet, and correspond to different impurity phases. The dark background indicates that no other strong CL emissions originate from the rest of the material. An area containing several occurrences of the three colours of emissive particles was selected on the basis of the optical CL images (Fig. 4a) and subsequently located in the SEM (Fig. 4b) in order that EDX microanalysis could be carried out on the luminescent particles.

In many cases, it was possible to correlate the CL emissions with specific, individual, grains in the microstructure. The compositions of the particles corresponding to the luminescent spots were matched to the colours observed under the optical microscope. It was found that each colour of emission corresponded to a distinct secondary phase, suggesting that optical CL

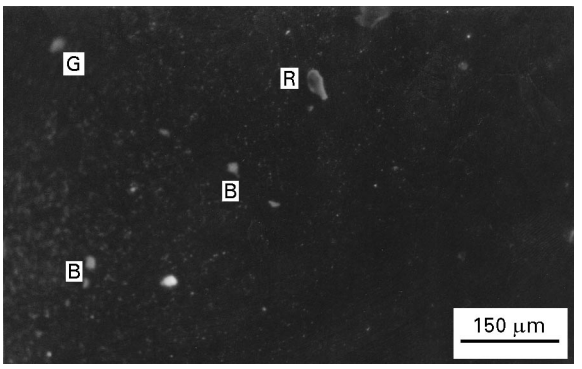

Figure 3 Optical CL image showing a number of bright spots of different colours corresponding to impurity phases. G = Green, R = Red and B = Blue.

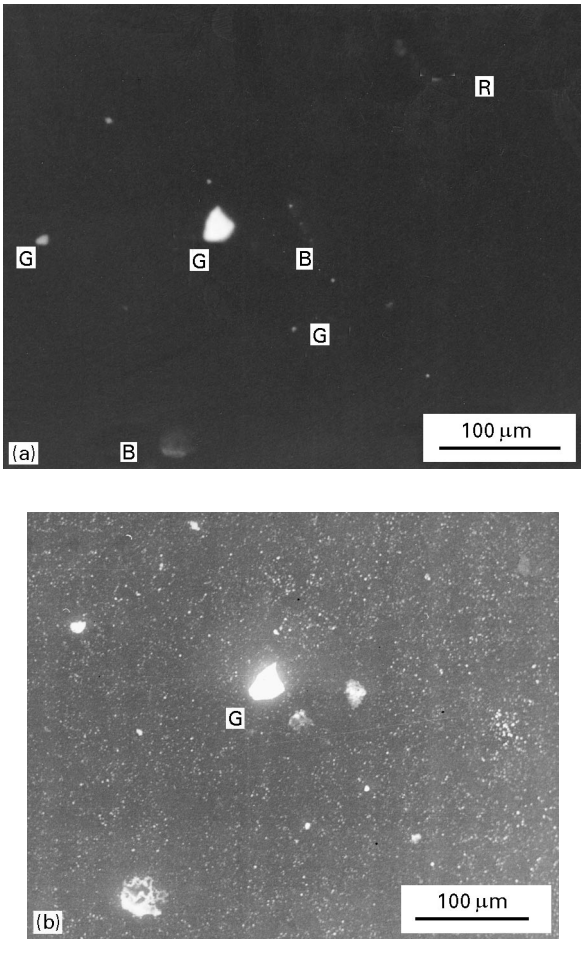

Figure 4 (a) Optical CL image of the area selected for detailed study G = Green, R = Red and B = Blue and (b) a SEM-CL image of the same area.

microscopy may be used as a quick method of mapping out impurity phase distributions and densities. Table 1 shows the compositions obtained from each of the different coloured luminescent spots, calculated as an average of several analyses.

Fig. 5(a and b) are SE and SEM–CL images of a particle embedded in the sample surface which gave rise to a red CL spot. A series of EDX analyses traversing this particle are presented in Fig. 6a and show the impurity to be an alumina grain 5–10 μm

TABLE I EDX analysis data showing the compositions of the CL emissive areas and their colours along with the matrix components

Luminescence colour	wt %				
	ZrO_2	Y_2O_3	SiO_2	Al_2O_3	Ni
Red	1.86	0	0.11	94.93	3.1
Blue	14.73	1.59	79.74	1.36	2.58
Bright green	92.44	2.33	3.55	1.26	0.42
Dark matrix	80.95	8.66	3.67	1.46	5.26

across. This dimension corresponds well with the observed size of the CL emission. In this case the red colour of the emission is due to Cr doping of the alumina and corresponds to the 'ruby red' line, providing an effective finger print for this material.

Fig. 5(c and d) are SE and SEM–CL images from a blue spot. The luminescent region appears diffuse and uneven in intensity. EDX analyses traversing this region (Fig. 6b) show strong enrichment in silicon and the blue emission is therefore attributed to a silica rich phase, possibly glassy and occurring throughout the microstructure in patchy regions 20–30 μm in size.

Fig. 5(e and f) are SE and SEM–CL images of a green spot. In the SE image the area is seen to correspond to a region of increased porosity of 20–30 μm across. The EDX analysis linescan (Fig. 6c) shows a similar composition for this region compared with the matrix but with a decrease in yttrium and an increase in zirconium. It is well known that the monoclinic phase of zirconia is many times more luminescent than the doped tetragonal or cubic forms [12] and we interpret the origin of the CL signal to unstabilized, monoclinic zirconia in the microstructure resulting from a local reduction in the yttria distribution. The porosity in the microstructure is due to the poor sintering characteristics of unstabilized zirconia, particularly at the low temperatures employed in this study (1000°C) which were intended to limit grain growth but would also have the effect of minimizing yttria migration during sintering.

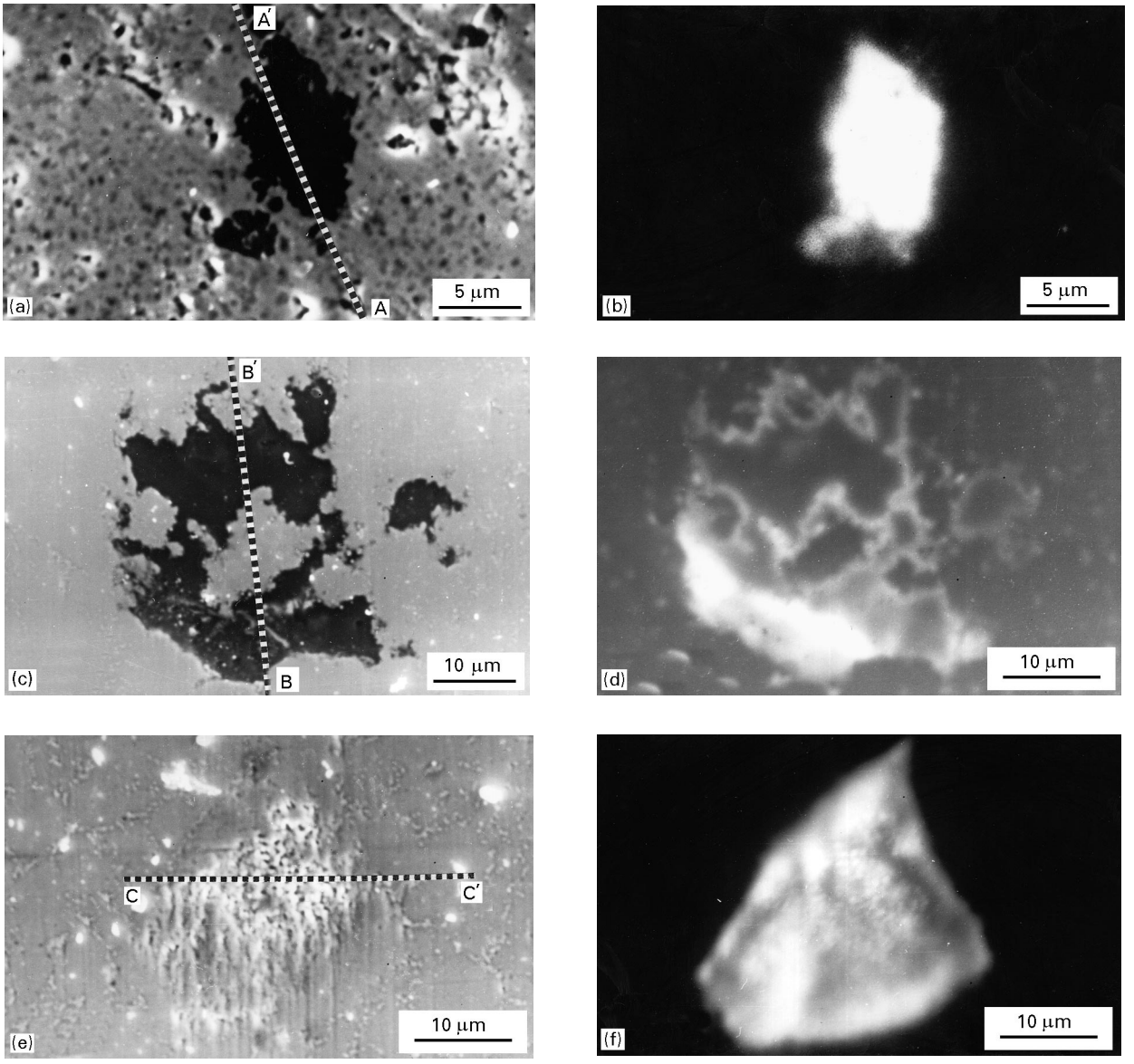

Figure 5 Secondary electron (a) and SEM-CL image of a red region (b). Secondary electron (c) and SEM-CL image of a blue region (d). Secondary electron (e) and (f) SEM-CL image of a green region. Fig. 5(a,c,e) show the lines of the EDX analyses presented in Figs 6(a–c).

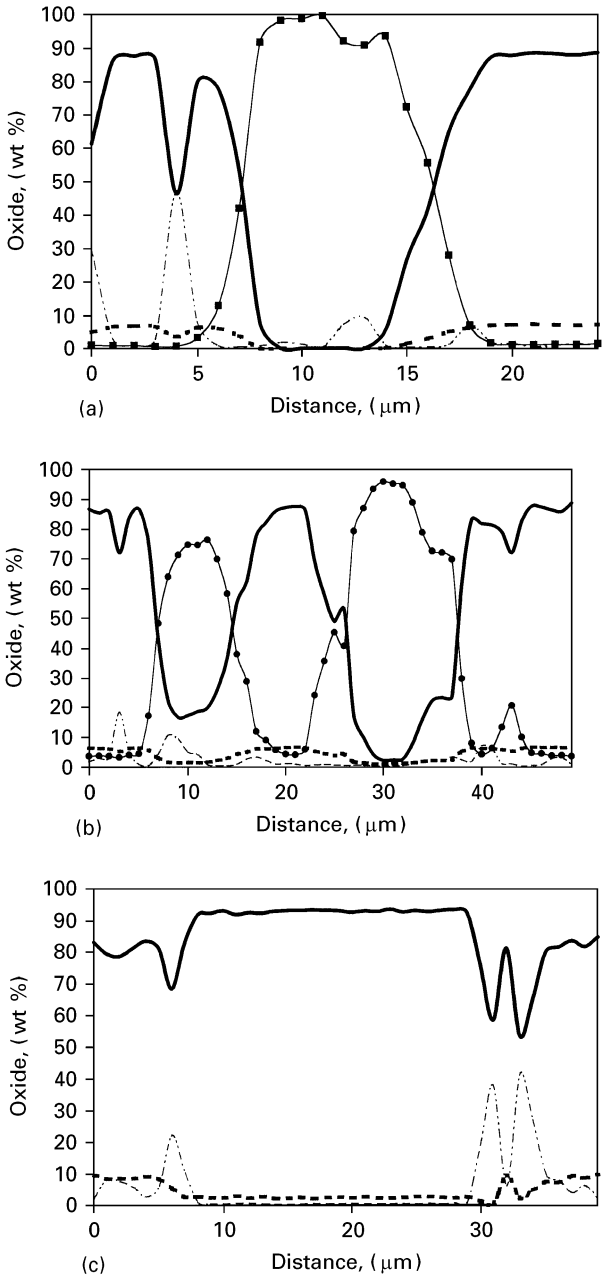

Figure 6 EDX linescan profiles of (a) a red spot along section A-A′ of Fig. 5(a) with (—) ZrO_2, (----) Y_2O_3, (–■–) Al_2O_3 and (–···–) Ni. Fig. 6b is a blue region along section B-B′ of Fig. 5c with (—) ZrO_2, (----) Y_2O_3, (–●–) SiO_2 and (–···–) Ni and Fig. 6c a green region along section C-C′ of Fig. 5e with (—) ZrO_2, (----) Y_2O_3 and (–···–) Ni.

At the sensitivities for detection used in this study the Ni particles and the cubic zirconia do not give rise to a strong CL signal, any luminescent phase detectable by CL is easily identified as either an impurity or other heterogeneity, enabling a rapid evaluation of any specimens prepared. It should be borne in mind that other undesirable, but non-strongly-luminescent, phases may be present in the microstructure in which case they will not be easily detected by CL analysis although at higher levels of sensitivity differences in CL spectra between less luminescent phases are likely to become apparent.

It should be noted that the precise colour of the CL emission (spectral CL response) in ceramics and wide band gap materials is primarily a function of the extra states introduced into the band gap by defects and impurities, and the presence of self luminescent centres. Within a given batch of material, for each phase these properties are likely to be sufficiently similar to have its own characteristic CL emission. This permits phase distributions of the type discussed here to be monitored easily. Within a material of different origin, however, it may be that there is a different population of CL active sites in the phase of interest and that the overall response is different. Care should therefore also be taken in assigning a particular spectral CL response to a specific phase when studying a new material prior to confirmation by EDX analysis.

4. Conclusions

It has been demonstrated that optical CL microscopy can be used to monitor impurity distributions in order to carry out quality control in appropriate materials. In the case described here the CL emission intensities from cubic-ZrO_2 and metallic Ni matrix phases are low and so strong emissions can be used directly to identify regions of heterogeneity in the microstructure. EDX analysis can then be used to identify the secondary phases highlighted by CL microscopy.

Acknowledgement

AG acknowledges financial support from BRITE/EURAM Grant BE 5564.

References

1. E. H. LUTZ, *J. Amer. Ceram. Soc.* **77** (1994) 1901.
2. M. P. HARMER, H. M. CHAN and G. A. MILLER, *J. Amer. Ceram. Soc.* **75** (1992) 1715.
3. R. W. DAVIDGE, "Mechanical Behaviour of Ceramics" (Cambridge University Press, 1979) p. 111.
4. P. R. FLETCHER and C. LEACH, *J. Mater. Sci.* **28** (1993) 6774.
5. D. J. MARSHALL, "Cathodoluminescence of Geological Materials" (Unwin Hyman Ltd., London 1988) p. 37.
6. D. B. HOLT, "Microscopy of Semiconducting Materials" (IOP, Bristol, 1981).
7. B. G. YACOBI and D. B. HOLT, "Cathodoluminescence Microscopy of Inorganic Solids" (Plenum Press, New York 1990).
8. J. T. CZERNUSKA and T. F. PAGE, *J. Amer. Ceram. Soc.* **68** (1985) C196.
9. C. LEACH and C. E. NORMAN, *J. Mater. Sci.* **30** (1995) 2799.
10. P. R. FLETCHER and C. LEACH, *J. Europ. Ceram. Soc.* **15** (1995) in press.
11. D. SPORN, "Development of nano–structured functional ceramic/metal composites", (Brite/Euram Project 5564 BRE2-0252, Fourth intermediate report, Fraunhofer-Institut für Silicatforschung, Würzburg, Germany, 1994) p. 17.
12. C. LEACH and C. E. NORMAN, *J. Mater. Sci.* **24** (1992) 4219.

Received 3 October
and accepted 20 November 1995